Structural Engineering and Mechanics, *Vol. 73, No. 2 (2020) 209-223*
DOI: https://doi.org/10.12989/sem.2020.73.2.209

Buckling of carbon nanotube reinforced composite plates supported by Kerr foundation using Hamilton's energy principle

Ammar Boulal[1], Tayeb Bensattalah[2,3], Abdelkader Karas[2], Mohamed Zidour*[2,3], Houari Heireche[1] and E.A. Adda Bedia[4]

[1]Laboratory de Modélisation et simulation Multi-échaelle,Département de physique, Faculté des Science Exactes Université de sidi Bel Abbés, Algeria
[2] Université Ibn Khaldoun, BP 78 Zaaroura, 14000 Tiaret, Algeria
[3] Laboratory of Geomatics and Sustainable Development, IbnKhaldoun University of Tiaret, Algeria
[4]Department of Civil and Environmental Engineering, King Fahd University of Petroleum & Minerals, 31261 Dhahran, Eastern Province, Saudi Arabia

(Received September 25, 2018, Revised July 26, 2019, Accepted October 5, 2019)

Abstract. This paper investigates the buckling behavior of carbon nanotube-reinforced composite plates supported by Kerr foundation model. In this foundation elastic of Kerr consisting of two spring layers interconnected by a shearing layer. The plates are reinforced by single-walled carbon nanotubes with four types of distributions of uniaxially aligned reinforcement material. The analytical equations are derived and the exact solutions for buckling analyses of such type's plates are obtained. The mathematical models provided, and the present solutions are numerically validated by comparison with some available results in the literature. Effect of various reinforced plates parameters such as aspect ratios, volume fraction, types of reinforcement, parameters constant factors of Kerr foundation and plate thickness on the buckling analyses of carbon nanotube-reinforced composite plates are studied and discussed.

Keywords: buckling; plate; Kerr foundation; reinforcement material; nanotube of carbon; volume fraction

1. Introduction

The continuum mechanics methods are widely used to predict the responses of micro and nano structure such as bending, buckling, vibration responses and functionally graded reinforcement (Meziane *et al*. 2014, Al-Basyouni *et al*. 2015, Bounouara *et al*. 2016, El-Haina *et al*. 2017, Kolahchi *et al*. 2017,Bellifa *et al*. 2017a, Kaci *et al*. 2018, Bouhadra *et al*. 2018, Bouadi *et al*. 2018, Karami*et al*. 2018a, Fourn *et al*. 2018, Cherif *et al*. 2018, Karami *et al*. 2019ab, Berghouti *et al*. 2019, Alimirzaei *et al*. 2019, Meksi *et al*. 2019, Chemi *et al*. 2018, Guessas *et al*. 2018, Hamidi *et al*. 2018, Rakrak *et al*. 2016, Tlidji *et al*. 2019).

Currently, the carbon nanotube-reinforced composites (CNTRCs) resting on the elastic medium is the main subject of many investigators; it has been utilized in an increasing number of industrial applications including aircraft, military, building and other civil structures, transportation, automotive, marine, machine elements and mechanical, sporting goods, chemical industries, biomedical applications, energy, infrastructure sectors, electrical, electronics and communication applications and it open up totally new horizons in a variety of industrial applications, compared with conventional materials.(Coleman *et al* 2006, Spitalsky *et al* 2010). This is due to their excellent properties of carbon nanotube (Pradhan and Phadikar 2009, Dihaj *et al*. 2018, Draoui *et al*. 2019, Medani *et al*. 2019), high specific strength (strength to weight ratio), due to which there is improvement in fuel efficiency, high durability, light weight, design and process flexibility, high resistance to damage, high resistance to corrosion, bio-degradation and extreme environmental conditions,… etc. Although studies on the mechanical, electrical, and thermal properties of carbon nanotube-reinforced composites (CNTRCs) have given important information and valued predictions, the ultimate purpose for the development of these materials is their applications in actual structures. Therefore, the global behavior of structural elements made of the CNTRCs should be considered for accurate predictions and optimal design (Hoang 2016).

The first work on carbon nanotube-reinforced composites (CNTRCs) ismade from polymer and aligned CNT investigated by Ajayan *et al* (1994). And since then many researchers have paid their attention on investigating material properties of the CNTRCs (Odegard*et al*. 2003, Mokashi 2007, Fadelus 2005, Hu 2005, Moradi-Dastjerdi 2016, Kolahchi *et al*. 2015). By using molecular dynamics (MD), the elastic properties of CNTRCs can be evaluated by (Han and Elliott 2007). Zhu *et al*. (2007) presented the stress-strain curves of CNT-reinforced composites, which show that the mechanical, electrical and thermal properties of the composite materials can be improved considerably with the addition of small amounts of CNTs to polymer matrix. In order to understand more about how to enhance dispersion and alignment of CNTs in a polymer matrix, Xie

*Corresponding author, Professor
E-mail: zidour.m@univ-tiaret.dz

http://www.techno-press.com/journals/sem&subpage=7
ISSN: 1225-4568 (Print), 1598-6217 (Online)

et al. (2005) reported the existing techniques used for this purpose.

In actual structural applications, and based on several benefits of CNTRCs as discussed above, these can be incorporated in the structural elements such as beams, plates and shells. To investigate mechanical behavior of engineering structures made from CNTRCs, there are a limited number of previous reports regarding mechanical responses of the CNTRC structures under different loading. In general, the problem of weak interfacial bonding between CNTs and polymer can occur in CNTRC structures. However, this problem can be solved by varying the CNTs within homogeneous matrix over the gradient direction(Shen 2009). In particular, several methods and theory are used with successfully for analysis the behaviour of CNTRCs under different loading which are treated as beams, thin shells or solids in cylindrical shapes and plates (Yas *et al*. 2012, Wattanasakulpong and Ungbhakorn2013, Ke *et al*. 2010, Zhu *et al*. 2012, Lei *et al*. 2013, Shen and Zhang 2010). For example, Kolahchi*et al*. (2017) studied the wave propagation of embedded viscoelastic FG-CNT-reinforced sandwich plates integrated with sensor and actuator based on refined zigzag theory. Mehar*et al* (2017a) analyzed the thermoelastic nonlinear frequency of CNT reinforced functionally graded sandwich structure, then Mehar *et al*. (2017) analyzed the FG-CNT reinforced shear deformable composite plate under various loading. Stability of CNTRCs plates and beams under thermal loads has been investigated in some works. (Shafiei and Setoodeh 2017,Shokravi 2017). In last years, many test problems and methods with more complexities are used. Kolahchi *et al*. (2015) analyzed a nonlocal nonlinear for buckling in embedded FG-SWCNT-reinforced microplates subjected to magnetic field. Thermal vibration of embedded FG nanoplates under non-uniform temperature distributions with different boundary conditions has given by Barati and Shahverdi (2016). Bouiadjra *et al*. (2013) studied the nonlinear thermal buckling behavior of FG-plates using an efficient sinusoidal shear deformation theory. Khayat *et al*. (2018) analyzed the vibration of functionally graded cylindrical shells with different shell theories using semi-analytical method. Ilati, and Dehghan (2015). Used the radial basis functions (RBFs) collocation and RBF-QR methods for solving the coupled nonlinear sine-Gordon equations.

The problem of beams on deformable foundation is the most commonly encountered problem and has many applications in engineering and science. Even though the continuum mechanics approach yields the most comprehensive data on the mechanical behaviors of various structures under foundation system, this lies in the fact that considerable experience of comparison between various foundation models are required.

In the Winkler foundation model, a set of independent springs formed the foundation system. The most rudimentary model has been widely adopted in studying the problem of structures on elastic foundation. The neglect of the existence of shear stress inside the foundation medium and the uncoupling of the individual Winkler foundation springs leads to an unrealistic abrupt change in the foundation surface displacement between the loaded and the unloaded regions. Pasternak foundation so called “two-parameter” assumes the existence of shear interactions between the spring elements. This may be accomplished by connecting the ends of the springs to a structure consisting of incompressible vertical elements, which deforms only by transverse shear.

In most applications, the CNTRC plate is resting on elastic foundation medium. The simplest and first type of elastic foundation is presented by Winkler as the “one-parameter” foundation model since it is characterized only by the vertical stiffness of the Winkler foundation springs (Zhang 2015, Dehghan and Baradaran 2011). In fact, both the first type of elastic foundation and the second type presented by Pasternak were introducing the second foundation parameter to account for the existence of shear stress inside the foundation medium, resulting in the so called “two-parameter” foundation model (Nguyen 2017,Thai and Choi 2011, Wattanasakulpong and Chaikittiratana 2015, Shen and Zhu 2012).

To further improve the two-parameter foundation model, (Kerr 1965) had studied a new foundation based on three foundation parameter so-called “three-parameter” foundation model. The major role of this model is to provide more flexibility in controlling the degree of foundation-surface continuity between the loaded and the unloaded regions of the structure-foundation system. Furthermore, for several types of foundation materials, neither the Winkler-foundation model nor the two-parameter foundation model can realistically represent the interaction mechanisms between the beams and the contacting media (Kerr 1964).

The Kerr-type foundation model is of particular interest since it stems from the famous Winkler Pasternak two-parameter foundation model for which the foundation medium is visualized as consisted of lower and upper spring separated by incompressible shear layer. The Kerr-type foundation model is characterized by three parameters the lower and upper spring moduli and the shear-layer section modulus.

Even though the Kerr-type foundation model was developed since the mid-sixties, there have been only a limited number of researchers studying the problem of beams resting on Kerr-type foundation. However, it is found that various theory based investigations concerned with the buckling of CNTs embedded in polymer matrix resting in Kerr’s foundation are rare in the literature.

To formulate the closed-form solutions of simply supported CNTRC plates, the Navier method is employed. In 1820, Navier presented a paper to the French Academy of Sciences on the solution of bending of simply supported rectangular plates by double trigonometric series. Navier’s solution is sometimes called the forced solution of the differential equations since it “forcibly” transforms the differential equation into an algebraic equation, thus considerably facilitating the required mathematical operations. various numerical methods are using to predict the linear and nonlinear problems appeared in physical, chemistry, mechanics and engineering applications such as: finite element meth, spectral element methods (Dehghan *et* *al*. 2016), method of variably scaled radial kernels (Dehghan and Mohammadi 2015a, Dehghan and Mohammadi 2015b), meshless techniques (Dehghan and Abbaszadeh 2019, Dehghan and Abbaszadeh 2016). Dehghan and Shokri (2008) used a numerical method for solution of the two-dimensional sine-Gordon equation using the radial basis functions. Dehghan *et al*. (2016) used legendre spectral element method for solving time fractional modified anomalous subdiffusion equation.

The main objective of this article is to investigate the buckling analyses of the simply supported CNTRC plates resting on the Kerr elastic foundation and to estimate the accuracy of the present foundation model compared to other models. The governing equations are derived by using Hamilton's principle and the exact solutions for buckling analyses of such type's plates are obtained. The mathematical models provided and the present solutions are numerically validated by comparison with some available results in the literature. Effect of various parameters of reinforced plates such as aspect ratios, volume fraction, types of reinforcement, parameters constant factors of Kerr's foundation and plate thickness on the buckling analyses of carbon nanotube-reinforced composite plates are studied and discussed. Thus, this paper can naturally be considered as a companion paper to the work on the plate-Kerr foundation system rarely used in the literature.

2. CNTRC-plates

Consider a CNTRC-plate having length (a), width (b) and thickness (h) which is resting on the Kerr elastic foundation, including shear layer and two Winkler springs, as shown in Fig. 1(a). The CNTRC-plates considered in this investigation are assumed to be reinforced by four different patterns of carbon nanotube distribution across the plate thickness, which can be seen in Fig. 1(b). It can be seen that UD-CNTs has uniform distribution of single-walled carbon nanotubes (SWCNTs); while, O-CNTs and X- CNTs have symmetrically distributed.

Two kinds of CNTRC-plate, namely, uniformly distributed (UD) and functionally graded (FG) reinforced with aligned carbon nanotube, are considered. The material properties of FG-CNTRC face sheets are assumed to be graded in the thickness direction. The load transfer between the nanotube and polymeric phases is less than perfect (e.g. the surface effects, strain gradients effects, intermolecular coupled stress effects, etc.). Hence, we introduce the CNT efficiency parameter (η_1, η_2, η_3) into Eq. (1) to consider the size-dependent material properties. The values of the CNT efficiency parameter is estimated by matching the elastic modulus of CNTRCs observed from the molecular dynamics (MD) simulation results with the numerical results obtained from the extended rule of mixture.

By using the rule of mixture, the effective material properties of CNTRC-plates made from a mixture of SWCNTs and an isotropic polymer matrix can be estimated. This rule includes the CNT efficiency parameters (η_1, η_2, η_3) in order to account for the scale-dependent material properties (Han and Elliott 2007). Thus, the material properties of the CNTRC-plates can be expressed as follows (Shen 2009).

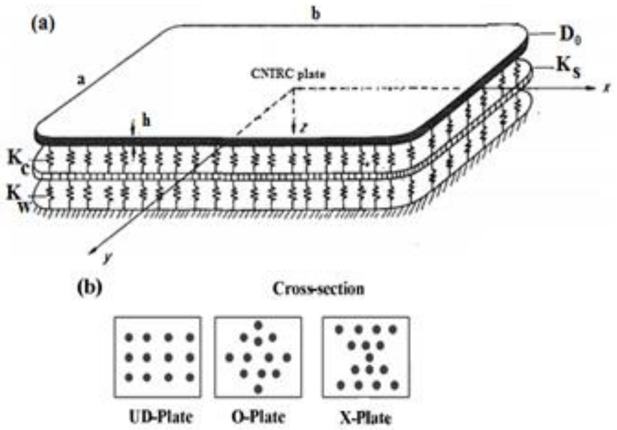

Fig. 1 Geometry of a CNTRC-plate supported by Kerr foundation model (a) and cross-sections with different patterns of carbon nanotube reinforcement (b)

$$E_{11} = \eta_1 V_{cnt} E_{11}^{cnt} + V_p E^p \tag{1a}$$

$$\frac{\eta_2}{E_{22}} = \frac{V_{cnt}}{E_{22}^{cnt}} + \frac{V_p}{E^p} \tag{1b}$$

$$\frac{\eta_3}{G_{12}} = \frac{V_{cnt}}{G_{12}^{cnt}} + \frac{V_p}{G^p} \tag{1c}$$

It is defined that $E_{11}^{cnt}, E_{22}^{cnt}$ are the Young's modulus and G_{12}^{cnt} indicate the Young's moduli and shear modulus of SWCNTs, respectively, and E^P and G^P represent the properties of the isotropic matrix. η_1, η_2 and η_3 are CNT/matrix efficiency parameters, The V_{cnt} and V_P are the volume fractions of the carbon nanotubes and matrix, respectively, and it is noticeable that the sum of the volume fractions of the two constituents equals to unity. For other properties in terms of Poisson's ratio (ν) and mass density (ρ), these can be written as:

$$\nu_{12} = V_{cnt}\nu_{12}^{cnt} + V_p \nu^p \;, \; \rho = V_{cnt}\rho^{cnt} + V_p \rho^p \tag{2}$$

To consider the CNTRC-plates with three patterns of reinforcement over the plate thickness, the mathematical models used for describing the material distributions can be written as (Zhu *et al*. 2012, Bakhadda *et al*. 2018):

UD- CNTs $$V_{cnt} = V_{cnt}^{*} \tag{3a}$$

O- CNTs $$V_{cnt} = 2\left(1 - 2\frac{|z|}{h}\right)V_{cnt}^{*} \tag{3b}$$

X- CNTs $$V_{cnt} = 4\left(\frac{|z|}{h}\right)V_{cnt}^{*} \tag{3c}$$

where V_{cnt}^{*} is the given volume fraction of CNTs, which can be obtained from the following equation:

$$V_{cnt}^{*} = \frac{W_{cnt}}{W_{cnt} + \left(\rho^{cnt}/\rho^{m}\right)\left(1 - W_{cnt}\right)} \tag{4}$$

Where W_{cnt} is the mass fraction of the carbon nanotube in the nano-composite plate, in this study, the CNT efficiency parameters (η) associated with the given volume fraction (V_{cnt}^{*}) are (Zhu *et al*. 2012):

$\eta_1 = 0.149$ and $\eta_2 = \eta_3 = 0.934$ for the case of $V_{cnt}^{*} = 0.11$

$\eta_1 = 0.150$ and $\eta_2 = \eta_3 = 0.941$ for the case of $V_{cnt}^{*} = 0.14$

$\eta_1 = 0.149$ and $\eta_2 = \eta_3 = 1.381$ for the case of $V_{cnt}^{*} = 0.17$

3.Equation of motion

The displacement field based on the theory of a material point located at (x, y, z) in CNTRC-plates is given below (Zenkour2006, Zenkour 2009, Mahi *et al*. 2015):

$$\begin{cases} u\left(x,y,z\right) = u_0\left(x,y\right) - z\,\dfrac{\partial w_0\left(x,y\right)}{\partial x} + \Psi\left(z\right)\varphi_x \\ v\left(x,y,z\right) = v_0\left(x,y\right) - z\,\dfrac{\partial w_0\left(x,y\right)}{\partial y} + \Psi\left(z\right)\varphi_y \\ w\left(x,y\right) = w_0\left(x,y\right) \end{cases} \tag{5}$$

It is noted that the displacement field in Eq. (5) can be easily adapted to various plate theories by choosing an appropriate shape function.

For example,

The classical plate theory (CPT) :

$$\Psi\left(z\right) = 0 \tag{6a}$$

The first order shear deformation theory (FSDT):

$$\Psi\left(z\right) = Z \tag{6b}$$

Third order shear deformation theory (TSDT):

$$\Psi\left(z\right) = z\left(1 - \frac{4z^2}{3h^2}\right) \tag{6c}$$

Sinusoidal shear deformation theory (SSDT):

$$\Psi\left(z\right) = \frac{h}{\pi}\sin\left(\frac{\pi z}{h}\right)_1 \tag{6d}$$

Exponential shear deformation theory (ESDT):

$$\Psi\left(z\right) = z \cdot e^{-2\left(z/h\right)^2} \tag{6d}$$

Hyperbolic shear deformation theory (HySDT)

$$\Psi\left(z\right) = h \cdot \tanh\left(\frac{z}{h}\right) - z\,\sec h^2\left(\frac{1}{2}\right) \tag{6d}$$

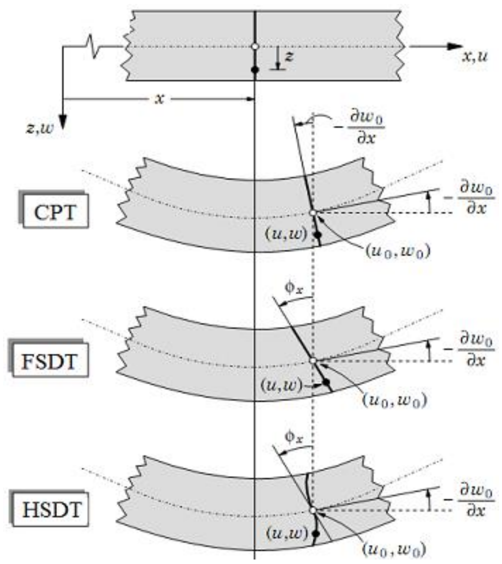

Fig. 2 Description of the plate deformation according to: classical (CLPT), first order (FSDT) and high order (HSDT) theories

In which u_0,v_0 and w_0 are the displacements along the x,y and z directions in the mid plane of the plate, ϕ_x , ϕ_y are the total bending rotation of the cross-section at any point of the reference plane (figure 2). If the last term in Eq. (5) is neglected, the displacements are reduced to the classical plate theory (CPT).

The linear in-plane and transverse shear strains are given by:

$$\begin{Bmatrix} \varepsilon_{xx} \\ \varepsilon_{yy} \\ \gamma_{xy} \end{Bmatrix} = \begin{Bmatrix} \dfrac{\partial u_0}{\partial x} \\ \dfrac{\partial v_0}{\partial y} \\ \dfrac{\partial u_0}{\partial y} + \dfrac{\partial v_0}{\partial x} \end{Bmatrix} - z\begin{Bmatrix} \dfrac{\partial^2 w_0}{\partial x^2} \\ \dfrac{\partial^2 w_0}{\partial y^2} \\ 2\dfrac{\partial^2 w_0}{\partial x \partial y} \end{Bmatrix} + \Psi(z)\begin{Bmatrix} \dfrac{\partial \phi_x}{\partial x} \\ \dfrac{\partial \phi_y}{\partial y} \\ \left(\dfrac{\partial \phi_x}{\partial y} + \dfrac{\partial \phi_y}{\partial x}\right) \end{Bmatrix} \tag{7a}$$

$$\begin{Bmatrix} \gamma_{xz} \\ \gamma_{yz} \end{Bmatrix} = \frac{\partial \Psi(z)}{\partial z}\begin{Bmatrix} \phi_x \\ \phi_y \end{Bmatrix} \tag{7b}$$

The expression of the constitutive relations is written in the form

$$\begin{Bmatrix} \sigma_{xx} \\ \sigma_{yy} \\ \sigma_{yz} \\ \sigma_{xz} \\ \sigma_{xy} \end{Bmatrix} = \begin{bmatrix} Q_{11} & Q_{12} & 0 & 0 & 0 \\ Q_{12} & Q_{22} & 0 & 0 & 0 \\ 0 & 0 & Q_{44} & 0 & 0 \\ 0 & 0 & 0 & Q_{55} & 0 \\ 0 & 0 & 0 & 0 & Q_{66} \end{bmatrix}\begin{Bmatrix} \varepsilon_{xx} \\ \varepsilon_{yy} \\ \varepsilon_{yz} \\ \gamma_{xz} \\ \gamma_{xy} \end{Bmatrix} \tag{8}$$

Where Q_{ij} are the transformed elastic constants

$$Q_{11} = \frac{E_{11}}{1 - \upsilon_{12}\upsilon_{21}},\quad Q_{22} = \frac{E_{22}}{1 - \upsilon_{12}\upsilon_{21}},\quad Q_{12} = \frac{\upsilon_{21}E_{11}}{1 - \upsilon_{12}\upsilon_{21}}$$

$$Q_{66} = G_{12}, \quad Q_{55} = G_{13}, \quad Q_{44} = G_{23}$$

$$G_{13} = G_{23} = G_{12} = \frac{\eta_3}{\left(\dfrac{V_{cnt}}{G_{12}^{cnt}} + \dfrac{V_p}{G^p}\right)}$$

Hamilton's principle is one of the variational principles in mechanics. All the laws of mechanics can be derived by using the Hamilton's principle. Hence it is one of the most fundamental and important principles of mechanics and mathematical physics. The Hamilton's principle is applied to produce the energy equations (Attia *et al*. 2015 and 2018, Abdelaziz *et al*. 2017, Belabed *et al*. 2018, Bourada *et al*. 2018 and 2019, Chaabane *et al*. 2019).

$$\int_0^t \left(\delta U_s + \delta U_f + \delta V \right) dt = 0 \tag{9}$$

Where δU_s, δU_f and δV are the virtual variation of the strain energy, the virtual potential energy of elastic foundation and the virtual work done by external forces.

Firstly, the expression of the virtual strain energy is (Beldjelili *et al*. 2016, Bousahla *et al*. 2016, Menasria *et al*. 2017, Bellifa *et al*. 2017b, Boussoula *et al*. 2019):

$$\delta U = \int_{-h/2}^{h/2} \int_A \Big(\sigma_{xx}\delta\varepsilon_{xx} + \sigma_{yy}\delta\varepsilon_{yy} + \sigma_{xy}\delta\gamma_{xy} + \sigma_{yz}\delta\gamma_{yz} + \sigma_{xz}\delta\gamma_{xz} \Big) dA dx \tag{10}$$

By substituting Eq. (7) into Eq. (10), one obtains

$$\begin{aligned} \delta U = \int_A \Big\{ & N_{xx}\delta u_{0,x} - M_{xx}\delta\varphi_{x,x} + P_{xx}\delta\varphi_{x,x} + \\ & N_{yy}\delta v_{0,y} - M_{yy}\delta w_{0,yy} + +P_{yy}\delta\varphi_{y,y} + \\ & N_{xy}\left(\delta u_{0,y} + \delta v_{0,x}\right) - 2M_{xy}\delta w_{0,xy} + P_{xy}\delta\left(\varphi_{x,y} + \varphi_{x,y}\right) \\ & + R_{yz}\delta\varphi_y + R_{xz}\delta\varphi_x \Big\} dxdy \end{aligned} \tag{11}$$

Where stress resultants can be defined as follows:

$$\left(N_{xx}, N_{yy}, N_{xy}\right) = \int_{-h/2}^{h/2} \left(\sigma_{xx}, \sigma_{yy}, \sigma_{xy}\right) dz \tag{12a}$$

$$\left(M_{xx}, M_{yy}, M_{xy}\right) = \int_{-h/2}^{h/2} z\left(\sigma_{xx}, \sigma_{yy}, \sigma_{xy}\right) dz \tag{12b}$$

$$\left(P_{xx}, P_{yy}, P_{xz}\right) = \int_{-h/2}^{h/2} \Psi(z)\left(\sigma_{xx}, \sigma_{yy}, \sigma_{xy}\right) dz \tag{12c}$$

$$\left(R_{xz}, R_{yz}\right) = \int_{-h/2}^{h/2} \frac{\partial \Psi(z)}{\partial z}\left(\sigma_{xz}, \sigma_{yz}\right) dz \tag{12d}$$

By substituting Eq. (8) into Eq. (12), one obtains the stress resultants in form of displacement components andmaterial stiffness.

$$\begin{Bmatrix} N_{xx} \\ N_{yy} \\ N_{xy} \end{Bmatrix} = \begin{bmatrix} A_{11} & A_{12} & 0 \\ A_{12} & A_{22} & 0 \\ 0 & 0 & A_{66} \end{bmatrix} \begin{Bmatrix} \varepsilon_{xx}^{(0)} \\ \varepsilon_{yy}^{(0)} \\ \gamma_{xy}^{(0)} \end{Bmatrix} + \begin{bmatrix} B_{11} & B_{12} & 0 \\ B_{12} & B_{22} & 0 \\ 0 & 0 & B_{66} \end{bmatrix} \begin{Bmatrix} \varepsilon_{xx}^{(1)} \\ \varepsilon_{yy}^{(1)} \\ \gamma_{xy}^{(1)} \end{Bmatrix} + \begin{bmatrix} C_{11} & C_{12} & 0 \\ C_{12} & C_{22} & 0 \\ 0 & 0 & C_{66} \end{bmatrix} \begin{Bmatrix} \varepsilon_{xx}^{(\Psi)} \\ \varepsilon_{yy}^{(\Psi)} \\ \gamma_{xy}^{(\Psi)} \end{Bmatrix} \tag{13a}$$

$$\begin{Bmatrix} M_{xx} \\ M_{yy} \\ M_{xy} \end{Bmatrix} = \begin{bmatrix} B_{11} & B_{12} & 0 \\ B_{12} & B_{22} & 0 \\ 0 & 0 & B_{66} \end{bmatrix} \begin{Bmatrix} \varepsilon_{xx}^{(0)} \\ \varepsilon_{yy}^{(0)} \\ \gamma_{xy}^{(0)} \end{Bmatrix} + \begin{bmatrix} D_{11} & D_{12} & 0 \\ D_{12} & D_{22} & 0 \\ 0 & 0 & D_{66} \end{bmatrix} \begin{Bmatrix} \varepsilon_{xx}^{(1)} \\ \varepsilon_{yy}^{(1)} \\ \gamma_{xy}^{(1)} \end{Bmatrix} + \begin{bmatrix} E_{11} & E_{12} & 0 \\ E_{12} & E_{22} & 0 \\ 0 & 0 & E_{66} \end{bmatrix} \begin{Bmatrix} \varepsilon_{xx}^{(\Psi)} \\ \varepsilon_{yy}^{(\Psi)} \\ \gamma_{xy}^{(\Psi)} \end{Bmatrix} \tag{13b}$$

$$\begin{Bmatrix} P_{xx} \\ P_{yy} \\ P_{xy} \end{Bmatrix} = \begin{bmatrix} C_{11} & C_{12} & 0 \\ C_{12} & C_{22} & 0 \\ 0 & 0 & C_{66} \end{bmatrix} \begin{Bmatrix} \varepsilon_{xx}^{(0)} \\ \varepsilon_{yy}^{(0)} \\ \gamma_{xy}^{(0)} \end{Bmatrix} + \begin{bmatrix} E_{11} & E_{12} & 0 \\ E_{12} & E_{22} & 0 \\ 0 & 0 & E_{66} \end{bmatrix} \begin{Bmatrix} \varepsilon_{xx}^{(1)} \\ \varepsilon_{yy}^{(1)} \\ \gamma_{xy}^{(1)} \end{Bmatrix} + \begin{bmatrix} F_{11} & F_{12} & 0 \\ F_{12} & F_{22} & 0 \\ 0 & 0 & F_{66} \end{bmatrix} \begin{Bmatrix} \varepsilon_{xx}^{(\Psi)} \\ \varepsilon_{yy}^{(\Psi)} \\ \gamma_{xy}^{(\Psi)} \end{Bmatrix} \tag{13c}$$

$$\begin{Bmatrix} R_{xz} \\ R_{yz} \end{Bmatrix} = \begin{bmatrix} H_{44} & 0 \\ 0 & H_{55} \end{bmatrix} \begin{Bmatrix} \gamma_{xy}^{(0)} \\ \gamma_{xy}^{(0)} \end{Bmatrix} \tag{13d}$$

Where

$$\begin{cases} \varepsilon_{xx}^{(0)} = \dfrac{\partial u_0}{\partial x} \\ \varepsilon_{yy}^{(0)} = \dfrac{\partial v_0}{\partial x} \\ \gamma_{xy}^{(0)} = \dfrac{\partial u_0}{\partial y} + \dfrac{\partial v_0}{\partial x} \end{cases} ; \begin{cases} \varepsilon_{xx}^{(1)} = -\dfrac{\partial^2 w_0}{\partial x^2} \\ \varepsilon_{yy}^{(1)} = -\dfrac{\partial^2 w_0}{\partial y^2} \\ \gamma_{xy}^{(1)} = -2\dfrac{\partial^2 w_0}{\partial x \partial y} \end{cases} ;$$
$$\begin{cases} \varepsilon_{xx}^{(\Psi)} = \dfrac{\partial \varphi_x}{\partial x} \\ \varepsilon_{yy}^{(\Psi)} = \dfrac{\partial \varphi_y}{\partial y} \\ \gamma_{xy}^{(\Psi)} = \dfrac{\partial \varphi_x}{\partial y} + \dfrac{\partial \varphi_y}{\partial x} \end{cases} ; \begin{cases} \gamma_{xz}^{0} = \varphi_x \\ \gamma_{yz}^{0} = \varphi_y \end{cases} \tag{14}$$

ϕ_x ,ϕ_y are the total bending rotation of the cross-section at any point of the reference plane (figure 2)

And A_{ij}, B_{ij}, C_{ij}, D_{ij}, E_{ij}, F_{ij}, H_{ij}, are the material stiffness components, defined by

$$\left[A_{ij}, B_{ij}, D_{ij}\right] = \int_{-h/2}^{h/2} Q_{ij}\left[1, z, z^2\right] dz; \quad i, j = 1,2,6 \tag{15a}$$

$$\left[C_{ij}, E_{ij}, F_{ij}\right] = \int_{-h/2}^{h/2} \Psi(z) Q_{ij}\left[1, z, \Psi(z)\right] dz; \quad i, j = 1,2,6 \tag{15b}$$

$$H_{44} = \int_{-h/2}^{h/2} \left(\frac{\partial \Psi(z)}{\partial z}\right)^2 Q_{44} dz; \tag{15c}$$

$$H_{55} = \int_{-h/2}^{h/2} \left(\frac{\partial \Psi(z)}{\partial z} \right)^2 Q_{55} dz \tag{15d}$$

In this study, it is assumed that the CNTRC-plates are rested on the Kerr elastic foundation composing of two spring layers interconnected by a shearing layer (Kerr 1964, Vancauwelaert *et al*. 2002). Thus, to address this problem, the virtual potential energy resulting from the elastic foundation is required to be involved in this investigation which is:

$$\begin{aligned} \delta U_f = & \frac{1}{1+\frac{K_w}{K_c}} \int_A K_w w_0 \delta w_0 - \\ & K_s \left(\frac{\partial w_0}{\partial x} \frac{\partial \delta w_0}{\partial x} + \frac{\partial w_0}{\partial y} \frac{\partial \delta w_0}{\partial y} \right) dxdy \\ & - \frac{1}{1+\frac{K_w}{K_c}} \int \frac{K_s \cdot D_0}{K_c} \cdot \left(\frac{\partial^5 w_0}{\partial x^5} \frac{\partial \delta w_0}{\partial x} \right. \\ & +3 \frac{\partial^4 w_0}{\partial x^4} \frac{\partial^2 \delta w_0}{\partial y^2} + 3 \frac{\partial^4 w_0}{\partial y^4} \frac{\partial^2 \delta w_0}{\partial x^2} \\ & \left. + \frac{\partial^5 w_0}{\partial y^5} \frac{\partial \delta w_0}{\partial y} \right) dxdy. \end{aligned} \tag{16}$$

Where K_w, K_s and K_c are the spring layers constants of Winkler, Pasternak and Kerr, respectively, which can be obtained in dimensionless parameters:

$$\begin{aligned} & K_w = \frac{\beta_w D_0}{a^4}; K_c = \frac{\beta_c D_0}{a^4}; \\ & K_s = \frac{\beta_s D_0}{a^2}; D_0 = \frac{E^p h^3}{12\left[1-\left(\nu^p\right)^2\right]}; \end{aligned} \tag{17}$$

It is noted that β_w, β_c and β_s are the corresponding spring constant factors which are the given parameters.

For the CNTRC-plates under buckling loading, $N_x^0 = \gamma_x N_{cr}$ and $N_y^0 = \gamma_y N_{cr}$, the virtual work done by these external loading is,

$$\delta V = \int_A \left(N_x^0 \frac{\partial w_0}{\partial x} \frac{\partial \delta w_0}{\partial x} + N_y^0 \frac{\partial w_0}{\partial y} \frac{\partial \delta w_0}{\partial y} \right) dxdy \tag{18}$$

By substituting Eqs.(13), (16) and (17) into Eq. (9), Then, integrating by parts and collecting the coefficients of δu_0, δv_0, δw_0, $\delta \varphi_x$ and $\delta \varphi_y$, leads to the following equations of motion.

$$\delta u_0 : \frac{\partial N_{xx}}{\partial x} + \frac{\partial N_{xy}}{\partial y} = 0 \tag{19a}$$

$$\delta v_0 : \frac{\partial N_{yy}}{\partial y} + \frac{\partial N_{xy}}{\partial x} = 0 \tag{19b}$$

$$\begin{aligned} & \delta w_0 : \frac{\partial^2 M_{xx}}{\partial x^2} + \frac{\partial^2 M_{yy}}{\partial y^2} + 2 \frac{\partial M_{xy}}{\partial x \partial y} + \\ & \frac{1}{1+\frac{K_w}{K_c}} \left(K_w w_0 + K_s \left(\frac{\partial^2 w_0}{\partial x^2} + \frac{\partial^2 w_0}{\partial y^2} \right) + \right. \\ & \left. \frac{K_s D_0}{K_c} \left(\frac{\partial^6 w_0}{\partial x^6} + 3 \frac{\partial^6 w_0}{\partial x^4 \partial y^2} + 3 \frac{\partial^6 w_0}{\partial x^2 \partial y^4} + \frac{\partial^6 w_0}{\partial y^6} \right) \right) = 0 \end{aligned} \tag{19c}$$

$$\delta \varphi_x : \frac{\partial p_{xx}}{\partial x} + \frac{\partial P_{xy}}{\partial y} - R_{xz} = 0 \tag{19d}$$

$$\delta \varphi_y : \frac{\partial p_{yy}}{\partial y} + \frac{\partial P_{xy}}{\partial x} - R_{yz} = 0 \tag{19e}$$

The boundary conditions for present model supposed simply supported along all edges of the plates can be considered as:

$$u_0 = w_0 = \varphi_x = N_{yy} = M_{yy} = P_{yy} = 0 \quad \text{at} \quad y=0,b$$

$$v_0 = w_0 = \varphi_y = N_{xx} = M_{xx} = P_{xx} = 0 \quad \text{at} \quad x=0,a$$

To formulate the closed-form solutions buckling problem of simply supported CNTRC plates, the Navier method is employed. Following the Navier solution procedure, we assume the following solution form for the displacement functions expanded in double trigonometric series that satisfies the boundary conditions,

$$\begin{aligned} u_0(x,y,t) &= \sum_{M=1}^{\infty} \sum_{N=1}^{\infty} U_{MN} \cos(\alpha x) \sin(\zeta y) \\ v_0(x,y,t) &= \sum_{M=1}^{\infty} \sum_{N=1}^{\infty} V_{MN} \sin(\alpha x) \cos(\zeta y) \\ w_0(x,y,t) &= \sum_{M=1}^{\infty} \sum_{N=1}^{\infty} W_{MN} \sin(\alpha x) \sin(\zeta y) \\ \varphi_x(x,y,t) &= \sum_{M=1}^{\infty} \sum_{N=1}^{\infty} \Theta x_{MN} \cos(\alpha x) \sin(\zeta y) \\ \varphi_y(x,y,t) &= \sum_{M=1}^{\infty} \sum_{N=1}^{\infty} \Theta y_{MN} \sin(\alpha x) \cos(\zeta y) \end{aligned} \tag{20}$$

Where $\alpha = \frac{M\pi}{a}$ and $\zeta = \frac{N\pi}{b}. i = \sqrt{-1}$

Where U_{MN}, and V_{MN}, W_{MN}, Θx_{MN} and Θy_{MN} are arbitrary parameters.

Substituting the Eq. (20) into the Eq. (19), we get the below equations for any fixed value of m and n, for bucking problem, which are presented in the following matrix form:

$$\left(\begin{bmatrix} s_{11} & s_{12} & s_{13} & s_{14} & s_{15} \\ s_{12} & s_{22} & s_{23} & s_{24} & s_{25} \\ s_{13} & s_{23} & s_{33} & s_{34} & s_{35} \\ s_{14} & s_{24} & s_{34} & s_{44} & s_{45} \\ s_{15} & s_{25} & s_{35} & s_{45} & s_{55} \end{bmatrix} \right) \begin{Bmatrix} U_{MN} \\ V_{MN} \\ W_{MN} \\ \Theta_{xMN} \\ \Theta_{yMN} \end{Bmatrix} = \begin{Bmatrix} 0 \\ 0 \\ 0 \\ 0 \\ 0 \end{Bmatrix} \tag{21}$$

Where

$$s_{11} = -A_{11}\alpha^2 + A_{66}\zeta^2,\ \ s_{12} = s_{21} = -\alpha\zeta(A_{12} + A_{66}),$$
$$s_{13} = s_{31} = -B_{11}\alpha^3 + B_{12}\alpha\zeta^2 + 2B_{66}\alpha\zeta^2,$$
$$s_{14} = s_{41} = -C_{11}\alpha^2 - C_{66}\zeta^2, s_{15} = s_{51} = -C_{12}\alpha\zeta - C_{66}\alpha\zeta,$$
$$s_{21} = -A_{12}\alpha\zeta - A_{66}\alpha\zeta s_{22} = -A_{11}\zeta^2 - A_{66}\alpha^2,$$
$$s_{23} = s_{32} = B_{12}\alpha^2\zeta + B_{22}\zeta^3 + 2B_{66}\alpha^2\zeta,$$
$$s_{24} = s_{24} = -C_{12}\alpha\zeta - C_{66}\alpha\zeta, s_{25} = s_{52} = -C_{22}\zeta^2 - C_{66}\alpha^2,$$
$$s_{33} = -D_{11}\alpha^4 - 2D_{12}\alpha^2\zeta^2 - D_{22}\zeta^4 - 4D_{66}\alpha^2\zeta^2 + \frac{1}{1+\frac{K_w}{K_c}}\left(-K_w + K_s\left(\alpha^2+\zeta^2\right)\right) - \frac{1}{1+\frac{K_w}{K_c}}\left(\frac{K_s D_0}{K_c}\left(\alpha^6 + 3\alpha^4\zeta^2 + 3\alpha^2\zeta^4 + \zeta^6\right)\right) - N_x^0\alpha^2 + N_y^0\zeta^2, \tag{22}$$
$$s_{34} = s_{43} = E_{11}\alpha^3 + E_{12}\alpha\zeta^2 + 2E_{66}\zeta^4,$$
$$s_{35} = s_{53} = E_{12}\alpha^2\zeta^2 + E_{22}\zeta^3 + 2E_{66}\alpha^2\zeta,$$
$$s_{44} = -F_{11}\alpha^2 - F_{66}\zeta^2 - H_{44},\ \ s_{45} = s_{54} = -\alpha\zeta(F_{12} + F_{66}),$$
$$s_{55} = -F_{22}\zeta^2 - F_{66}\alpha^2 - H_{55}$$

The dimensionless parameters used to present the numerical results for buckling analyses of CNTRC plates is as follows.

$$\overline{N}_{cr} = \frac{N_{cr}a^4}{\pi^2 D_0} \tag{23}$$

5. Results and discussions

In this section, numerical results of the effect of various elastic foundation parameters of the Kerr's foundation, where the lower spring modulus parameter, the upper spring modulus parameter and the shear layer modulus parameter, on the dimensionless critical buckling loads of CNTRC-plates are presented and discussed. Note that for the results in Kerr's foundation tend to the results in Pasternak's foundation; for the results in Kerr's foundation tend to the results in Winkler's foundation. The effective material characteristics of CNTRC-plates employed throughout this work are given as follows.

Here, Poly (m-phenylenevinylene)(PMPV) is used as the matrix in which material properties are: v^P=0.34, ρ^P=1150 kg/m^3 and E^P =2.1GPa. For reinforcement material, the armchair (10,10) SWCNTs is chosen with the following properties according to the study of Zhu *et al*. (2012):

$$v_{12}^{cnt} = 0.175;\ \ \rho^{cnt} = 1400 kg/m^3;\ \ E_{11}^{cnt} = 5.6466 TPa;$$
$$E_{22}^{cnt} = 7.0800 TPa;\ \ \ G_{12}^{cnt} = G_{13}^{cnt} = G_{23}^{cnt} = 1.9445 TPa$$

The algorithm for the proposed procedure of model is given in Figure 3.

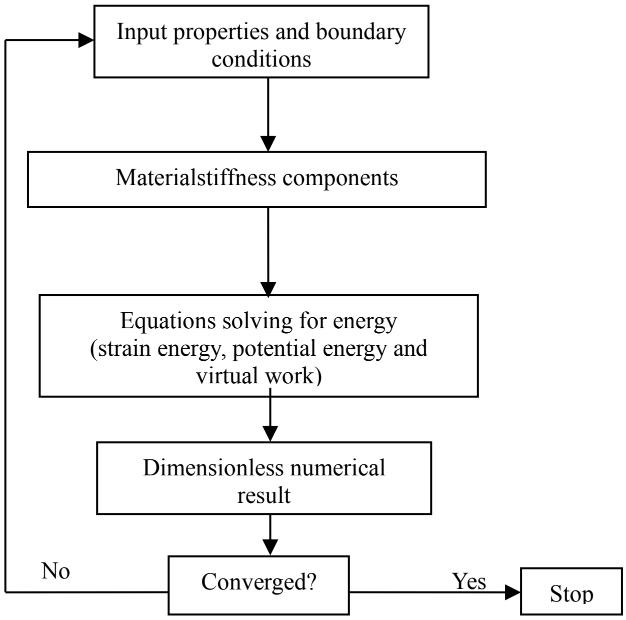

Fig. 3 The algorithm for the proposed procedure of model

In order to prove the validity of mathematical models in previous sections of the present theory, the results obtained are adopted and compared with the existing ones in the literature which were presented by Wattanasakulpongand Chaikittiratana, (2015) in Table1 and Guessas *et al*. (2018) in Table 2. With different patterns of carbon nanotube distribution, different values of carbon nanotube volume fraction and thickness ratio of plate (a/h=10). It can be observed from this comparison the good agreement between the present resultsand them obtained by Wattanasakulpong and Chaikittiratana, (2015) and Guessas *et al*. (2018). In addition, it is clearly seen that the CNTRC-plate with X-CNTscarbon nanotube distribution is defined as X-CNTs, shows its strongest capacity to resist the buckling load with the biggest values of dimensionless critical buckling loads, and followed by the UD-CNTs, and O-CNTs.

Table 3 presents the effect of elastic foundation on the dimensionless critical buckling loads $\overline{N}_{cr}$ for various types of CNTRC-plates subjected to uniaxial compression ($\gamma_x = -1, \gamma_y = 0$) and biaxial compression ($\gamma_x = -1, \gamma_y = -1$) with versus the CNT volume fraction associated with different values of spring constant factors, width thickness ratio of the plates is set to be (a/h = 10).The results show that the plates dimensionless critical buckling loads have a higher value when the volume fraction of CNT is larger, since the stiffness of CNTRC-plates is larger when the value of CNT volume fraction is higher. Moreover, for all different distributions of CNTs, FG-X plates have larger buckling load values than UD plates and values of FG-O plates are smaller than UD-CNTs plates. That is expected since CNT reinforcements distributed close to top and bottom are more efficient than those distributed near the mid-plane for increasing the stiffness of CNTRC plates by Zhu *et al* (2012). In addition, X-CNTs show its strongest capacity in resisting buckling load, and followed with UD- and O-CNTs, respectively. It is also observed that the spring constant factors have significant impact on the buckling loads of the plates, particularly when β_w, β_s and β_c are included. Obviously, the plates subjected to biaxial compressive loads have lower buckling results than those under uniaxial compressive loads.

Figs. 4–5 show the variation of the dimensionless critical buckling loads of various types of CNTRC-plates resting on the Kerr's foundation under uniaxial compression ($\gamma_x = -1, \gamma_y = 0$) and biaxial compression ($\gamma_x = -1, \gamma_y = -1$) with versus the CNT volume fraction at spring constant

Table 1 Comparisons of dimensionless critical buckling loads $\overline{N}_{cr}$ of CNTRC square plates with and without elastic foundation for uniform (UD-CNTs) and symmetric (X-CNTs, O-CNTs) distributed of (SWCNTs) at (a/h=10)

Uniaxial compression ($\boldsymbol{\gamma_x = -1, \gamma_y = 0}$)												
				$V_{cnt}^{*}=0.11$			$V_{cnt}^{*}=0.14$			$V_{cnt}^{*}=0.17$		
β_w	β_s	β_c	Theory	UD-CNTs	X-CNTs	O-CNTs	UD-CNTs	X-CNTs	O-CNTs	UD-CNTs	X-CNTs	O-CNTs
0	0	∞	Wattanasakulpong (2015) TSDT	20.68	24.29	14.50	23.36	26.89	16.70	32.32	37.69	22.68
			Wattanasakulpong (2015) SSDT	20.73	24.39	14.45	23.42	27.02	16.65	32.39	37.81	22.63
			Present ESDT	20.81	24.56	14.42	23.54	27.21	16.61	32.52	38.00	22.60
			PresentHySDT	20.71	24.36	14.46	23.40	26.97	16.66	32.36	37.77	22.64
100	0	∞	Wattanasakulpong (2015) TSDT	21.71	25.31	15.53	24.38	27.92	17.73	33.34	38.72	23.71
			Wattanasakulpong(2015) SSDT	21.76	25.42	15.48	24.45	28.04	17.67	33.42	38.83	23.65
			Present ESDT	21.84	25.58	15.45	24.56	28.23	17.64	33.54	39.03	23.62
			PresentHySDT	21.74	25.38	15.49	24.43	28.00	17.69	33.39	38.79	23.67
100	50	∞	Wattanasakulpong(2015) TSDT	31.84	35.45	25.66	34.51	38.05	27.86	43.48	48.85	33.84
			Wattanasakulpong (2015) SSDT	31.89	35.55	25.61	34.58	38.18	27.80	43.55	48.97	33.79
			Present ESDT	31.99	35.73	25.60	34.71	38.38	27.79	43.69	49.18	33.77
			PresentHySDT	31.89	35.53	25.64	34.57	38.15	27.83	43.54	48.94	33.82
Biaxial compression ($\gamma_x = -1, \gamma_y = -1$)												
0	0	∞	Wattanasakulpong(2015) TSDT	10.34	12.14	7.25	11.68	13.45	8.35	16.16	18.85	11.34
			Wattanasakulpong(2015) SSDT	10.36	12.20	7.23	11.71	13.51	8.32	16.19	18.90	11.31
			Present ESDT	10.41	12.28	7.21	11.77	13.60	8.31	16.26	19.00	11.30
			PresentHySDT	10.36	12.18	7.23	11.70	13.49	8.33	16.18	18.88	11.32
100	0	∞	Wattanasakulpong(2015) TSDT	10.85	12.66	7.76	12.19	13.96	8.86	16.67	11.85	19.36
			Wattanasakulpon (2015) SSDT	10.88	12.71	7.74	12.22	14.02	8.84	16.71	11.83	19.42
			Present ESDT	10.92	12.79	7.72	12.28	14.11	8.81	16.77	11.81	19.51
			PresentHySDT	10.87	12.69	7.75	12.21	14.00	8.84	16.69	11.83	19.39
100	50	∞	Wattanasakulpong (2015) TSDT	15.92	17.72	12.83	17.26	19.03	13.93	21.74	24.43	16.92
			Wattanasakulpong(2015) SSDT	15.94	17.78	12.81	17.29	19.09	13.90	21.77	24.48	16.89
			Present ESDT	16.13	18.00	12.93	17.49	19.32	14.03	21.98	24.72	17.02
			PresentHySDT	16.08	17.90	12.95	17.42	19.21	14.05	21.90	24.60	17.04

Table 2 Comparisons of dimensionless critical buckling loads of CNTRC square plates without elastic foundation and $\boldsymbol{V_{cnt}^{*} = 0.11}$

Uniaxial compression ($\boldsymbol{\gamma_x = -1, \gamma_y = 0}$)			
Theory	UD-CNTs	X-CNTs	O-CNTs
Guessas *et al*. (2018) FSDT	20.54	23.96	14.98
Present ESDT	20.81	24.56	14.42
PresentHySDT	20.71	24.36	14.46
Biaxial compression ($\boldsymbol{\gamma_x = -1, \gamma_y = -1}$)			
Guessas *et al*. (2018) FSDT	10.27	11.98	7.49
Present ESDT	10.41	12.28	7.21
PresentHySDT	10.36	12.18	7.23

factors (β_w, β_s and β_c=100) and a/b=3. It can be seen that as the width-to-thickness ratio of the plate increases, the non-dimensional buckling load parameters increase and buckling load parameters for all types of CNTRC plates increase also.

Figs. 6-7 show the variation of the dimensionless critical buckling loads of various CNTRC-plates types with plate aspect ratio (a/b) changing from 1.0 to 3.0. The plate width-to-thickness ratio (a/h) is set to be 10 resting on the Kerr's foundation (β_w, β_s and β_c=100) under uniaxial compression ($\boldsymbol{\gamma_x = -1, \gamma_y = 0}$) and biaxial compression ($\gamma_x = -1, \gamma_y = -1$) with versus the CNT volume fraction. It can be seen that buckling load parameters decrease as plate aspect ratio changes from 1.0 to 3.0. It is worth noting that the change of plate aspect ratio has a very small effect on buckling load parameter for CNTRC plates under biaxial compression.

Table 3 Effect of elastic foundation on the dimensionless critical buckling loads $\bar{N}_{cr}$ of CNTRC square plates for uniform (UD-CNTs) and symmetric (X-CNTs, O-CNTs) distributed of (SWCNTs) at (a/h=10)

Uniaxial compression ($\gamma_x = -1, \gamma_y = 0$)												
β_w	β_s	β_c		$V_{cnt}^{*}=0.11$			$V_{cnt}^{*}=0.14$			$V_{cnt}^{*}=0.17$		
			Present Theory	UD-CNTs	X-CNTs	O-CNTs	UD-CNTs	X-CNTs	O-CNTs	UD-CNTs	X-CNTs	O-CNTs
100	0	100	ESDT	21.33	25.07	14.93	24.05	27.72	17.13	33.03	38.52	23.11
			HySDT	21.22	24.87	14.98	23.91	27.49	17.17	32.88	38.28	23.16
100	0	200	ESDT	21.50	25.24	15.10	24.22	27.89	17.30	33.20	38.69	23.28
			HySDT	21.40	25.04	15.15	24.08	27.66	17.34	33.05	38.45	23.33
100	50	100	ESDT	46.13	49.88	39.74	48.86	52.53	41.93	57.83	63.32	47.91
			HySDT	46.03	49.68	39.78	48.72	52.29	41.98	57.68	63.08	47.96
100	50	200	ESDT	41.41	45.16	35.02	44.14	47.81	37.21	53.11	58.60	43.19
			HySDT	41.31	44.96	35.06	44.00	47.57	37.26	52.96	58.36	43.24
100	100	100	ESDT	70.94	74.68	64.54	73.66	77.33	66.74	82.64	88.13	72.72
			HySDT	70.84	74.48	64.59	73.52	77.10	66.78	82.49	87.89	72.77
100	100	200	ESDT	61.33	65.07	54.93	64.05	67.72	57.13	73.03	78.52	63.11
			HySDT	61.22	64.87	54.98	63.91	67.49	57.17	72.88	78.28	63.15
Biaxial compression ($\gamma_x = -1, \gamma_y = -1$)												
100	0	100	ESDT	10.66	12.53	7.466	12.025	13.86	8.563	16.514	19.259	11.55
			HySDT	10.61	12.43	7.489	11.956	13.74	8.586	16.438	19.139	11.57
100	0	200	ESDT	10.74	12.62	7.552	12.110	13.94	8.648	16.600	19.344	11.64
			HySDT	10.69	12.52	7.574	12.042	13.82	8.672	16.524	19.225	11.66
100	50	100	ESDT	20.70	22.57	17.509	22.067	23.90	18.60	28.917	31.661	23.95
			HySDT	20.65	22.47	17.531	21.999	23.78	18.62	28.841	31.542	23.98
100	50	200	ESDT	20.70	22.57	17.50	22.067	23.90	18.60	26.557	29.301	21.59
			HySDT	20.65	22.47	17.531	21.999	23.78	18.62	26.481	29.182	21.62
100	100	100	ESDT	35.46	37.34	32.272	36.830	38.66	33.36	41.320	44.064	36.36
			HySDT	35.41	37.24	32.294	36.761	38.54	33.39	41.243	43.944	36.38
100	100	200	ESDT	30.66	32.53	27.466	32.024	33.86	28.56	36.514	39.258	31.55
			HySDT	30.61	32.43	27.488	31.956	33.74	28.58	36.438	39.139	31.57

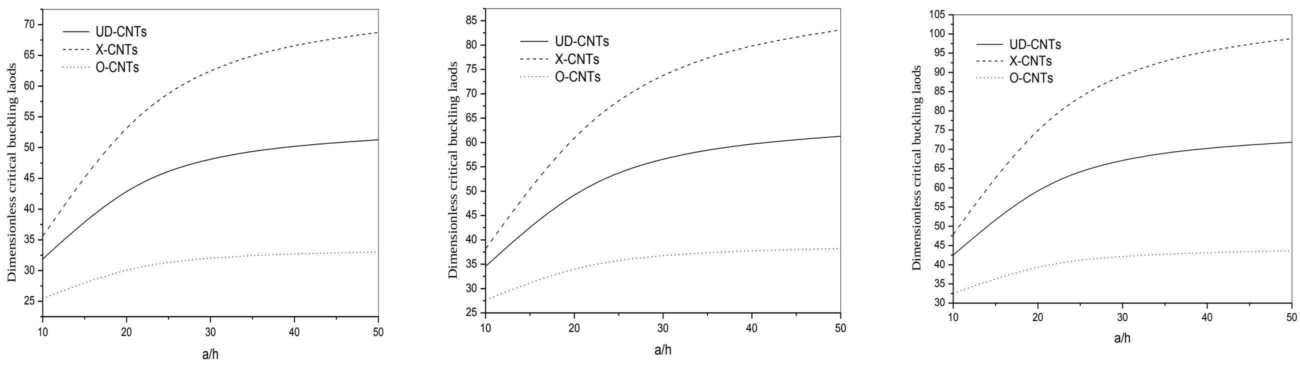

a) $V_{cnt}^{*}=0.11$ b) $V_{cnt}^{*}=0.14$ c) $V_{cnt}^{*}=0.17$

Fig. 4 Variation of the dimensionless buckling load parameter of simply supported various types of CNTRC plates versus the plate width-to-thickness ratio under uniaxial compression ($\gamma_x = -1, \gamma_y = 0$) with versus the CNT volume fraction

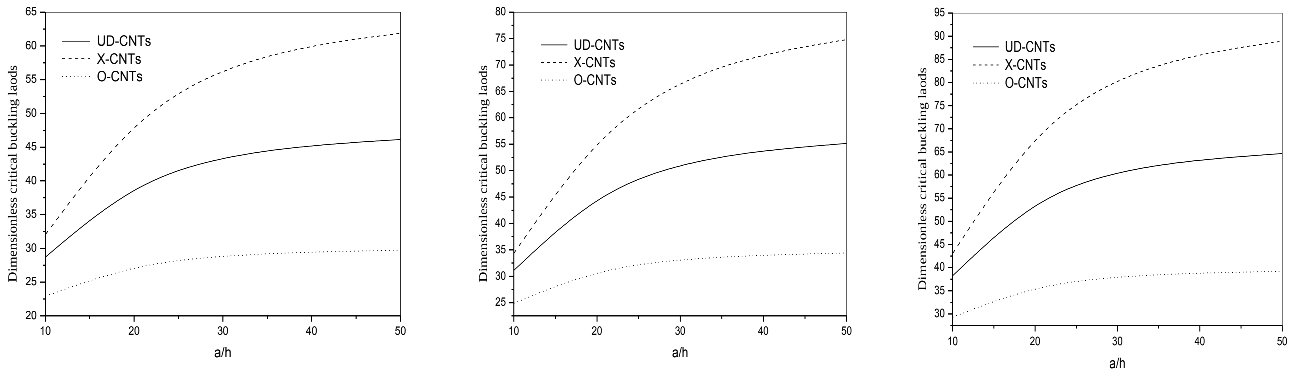

a) $V_{cnt}^{*}=0.11$ b) $V_{cnt}^{*}=0.14$ c) $V_{cnt}^{*}=0.17$

Fig.5 Variation of the dimensionless buckling load parameter of simply supported various types of CNTRC plates versus the plate width-to-thickness ratio under biaxial compression ($\gamma_x=-1, \gamma_y=-1$) with versus the CNT volume fraction

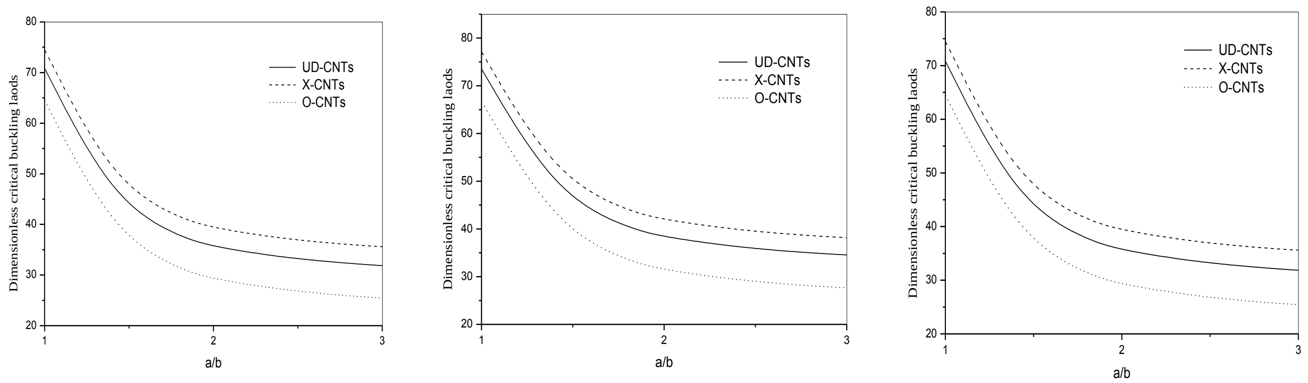

a) $V_{cnt}^{*}=0.11$ b) $V_{cnt}^{*}=0.14$ c) $V_{cnt}^{*}=0.17$

Fig. 6 Variation of the buckling load parameter of simply supported various CNTRC-plates types versus aspect ratio under uniaxial compression ($\gamma_x=-1, \gamma_y=0$) with versus the CNT volume fraction

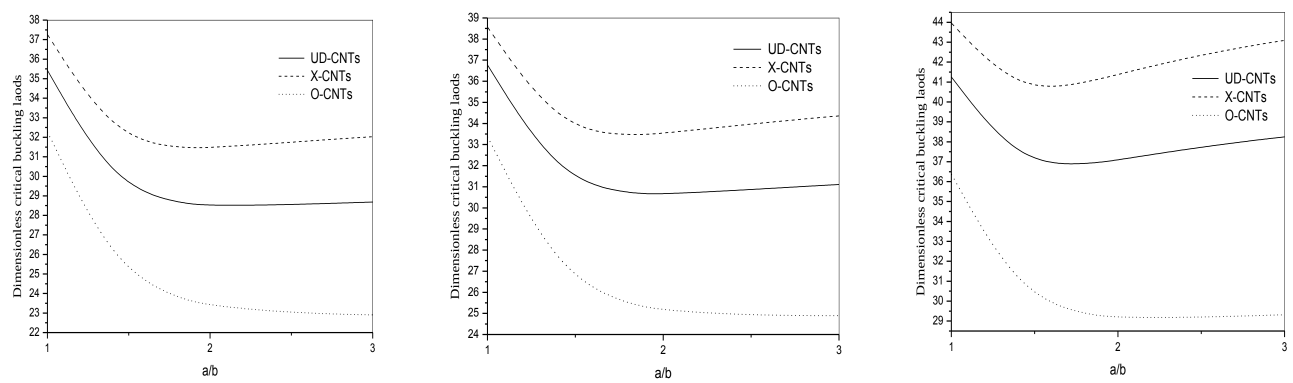

a) $V_{cnt}^{*}=0.11$ b) $V_{cnt}^{*}=0.14$ c) $V_{cnt}^{*}=0.17$

Fig. 7 Variation of the buckling load parameter of simply supported various CNTRC-plates types versus plate aspect ratio under biaxial compression ($\gamma_x=-1, \gamma_y=-1$) with versus the CNT volume fraction

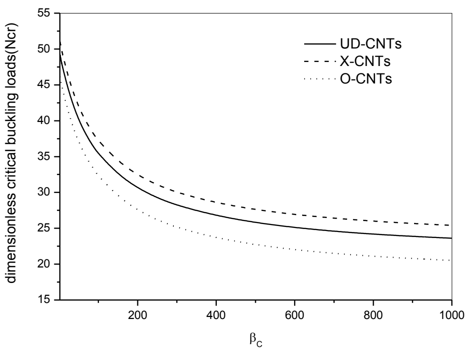

Fig. 8 Effect of Kerr's foundation parameter on dimensionless critical buckling loads of various square CNTRC-plates types with aspect ratio (a/h=10) and ($\beta_w = \beta_s$ = 100) under biaxial compression.

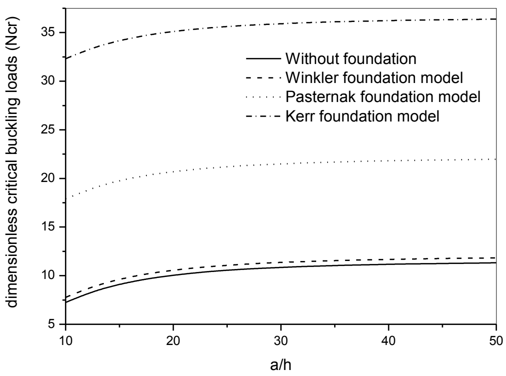

Fig. 9 Effect of various foundation model on dimensionless critical buckling loads of square CNTRC-plates with (O-CNTs) distribution under biaxial compression

Fig. 8shows the effect of kerr's modulus parameter on the dimensionless critical buckling load of different types of CNTRC- plate. It is observed that the dimensionless critical buckling loads decrease as the increase of the spring constant factors β_c. Note that for β_c =1000, the results in Kerr's foundation tend tothe results in Pasternak's foundation. In additional, the effect of various distributions of CNTs on the dimensionless critical buckling load is observed in the strongest (X-CNTs) and smallest (O-CNTs) values. It can be concluded that the difference between the effect of various distributions is attributed to a concentration of the carbone nanotube at the top and bottom face of plate.

Fig. 9 shows a comparison of dimensionless critical buckling load of square CNTRC-plates between various models of elastic medium with simply supported boundary conditions and (O-CNTs) distribution under biaxial compression.

It is observed that for various model of elastic medium the buckling load increases with small values as ratio L/h is varied from 10 to 50. In addition, it is observed that there is a significant influence of type of the elastic medium on the dimensionless critical buckling loads of square CNTRC-plates.

6. Conclusions

This article studies the buckling behavior of carbon nanotube-reinforced composite plates resting on the foundation elastic consisting of two spring layers interconnected by a shearing layerthat was suggested by (Kerr 1964). The plates are reinforced by single-walled carbon nanotubes with four distributions types of uniaxially aligned reinforcement material.

For this study, the results showed the dependence of buckling behavior on the different parameters such as aspect ratios, volume fraction, types of reinforcement and plate thickness. Besides on the results, it is observed for buckling analysis of such plates that the FG-X plates have larger buckling load values and its strongest capacity in resisting buckling load than UD plates and values of FG-O plates are smaller than UD plates. That is expected since CNT reinforcements distributed close to top and bottom are more efficient than those distributed near the mid-plane for increasing the stiffness of CNTRC plates. In addition, it is also observed that the spring constant factors have significant impact on the buckling loads of the plates, particularly when β_w, β_s *and* β_c are included. Obviously, the plates subjected to biaxial compressive loads have lower buckling results than those under uniaxial ones.

From the obtained results, it is concluded that the Kerr model is more accurate than the Winkler and the Pasternak models for the representation of the carbon nanotube-reinforced composite plates resting on the foundation elastic. The Kerr model is relatively simple to use and agrees well with the nonlocal elastic continuum model.An improvement of the present study will be considered in the future work to consider the stretching effect and other type of materials (Draiche *et al*. 2016, AitAtmane *et al*. 2017, Chikh *et al*. 2017, Karami *et al*. 2017, Abualnour *et al*. 2018, Karami *et al*. 2018bc, Zine *et al*. 2018, Yazid *et al*. 2018, Mokhtar *et al*. 2018, Benchohra *et al*. 2018, Younsi *et al*. 2018, Youcef *et al*. 2018, Addou *et al*. 2019, Boukhlif *et al*. 2019, Boulefrakh *et al*. 2019, Boutaleb *et al*. 2019, Khiloun *et al*. 2019, Draiche *et al*. 2019, Hellal *et al*. 2019, Hussain *et al*. 2019, Karami *et al*. 2019cd, Mahmoudi *et al*. 2019, Zaoui *et al*. 2019, Zarga *et al*. 2019).

Acknowledgments

Authors would like to acknowledge the support provided by the Directorate General for Scientific Research and Technological Development (DGRSDT).

References

Abdelaziz, H.H., Ait Amar Meziane, M., Bousahla, A.A., Tounsi, A., Mahmoud, S.R. and Alwabli, A.S. (2017), "An efficient hyperbolic shear deformation theory for bending, buckling and free vibration of FGM sandwich plates with various boundary conditions", *Steel Compos. Struct.*, **25**(6), 693-704. https://doi.org/10.12989/scs.2017.25.6.693.

Abualnour, M., Houari, M.S.A., Tounsi, A., AddaBedia, E.A., Mahmoud, S.R. (2018), "A novel quasi-3D trigonometric plate theory for free vibration analysis of advanced composite plates", *Compos. Struct.*, **184**, 688–697. https://doi.org/10.1016/j.compstruct.2017.10.047.

Addou, F.Y., Meradjah, M., M.A.A, Bousahla, Benachour, A., Bourada, F., Tounsi, A., Mahmoud, S.R. (2019), "Influences of porosity on dynamic response of FG plates resting on Winkler/Pasternak/Kerr foundation using quasi 3D HSDT", *Comput. Concrete*, **24**(4), 347-367. https://doi.org/10.12989/cac.2019.24.4.347.

AitAtmane, H, Tounsi, A., Bernard, F. (2017), "Effect of thickness stretching and porosity on mechanical response of a functionally graded beams resting on elastic foundations", *J. Mech. Mater. Design*, **13**(1), 71-84. https://doi.org/10.1007/s10999-015-9318-x.

Ajayan, P.M., Stephen, O., Colliex, C., Trauth, D. (1994), "Aligned carbon nanotube arrays formed by cutting a polymer resin-nanotube composite", *Science*, **256**, 1212-1214. https://doi.org/10.1126/science.265.5176.1212.

Al-Basyouni, K.S., Tounsi, A. and Mahmoud, S.R. (2015), "Size dependent bending and vibration analysis of functionally graded micro beams based on modified couple stress theory and neutral surface position", *Compos. Struct.*,**125**, 621-630. https://doi.org/10.1016/j.compstruct.2014.12.070.

Allahkarami, F., Nikkhah-Bahrami, M. and Saryazdi, M.G. (2017), "Damping and vibration analysis of viscoelastic curved microbeam reinforced with FG-CNTs resting on viscoelastic medium using strain gradient theory and DQM", *Steel Compos. Struct*., **25**(2), 141-155. https://doi.org/10.12989/scs.2017.25.2.141.

Alimirzaei, S., Mohammadimehr, M., Tounsi, A. (2019), "Nonlinear analysis of viscoelastic micro-composite beam with geometrical imperfection using FEM: MSGT electro-magneto-elastic bending, buckling and vibration solutions", *Struct. Eng. Mech.*, **71**(5), 485-502. https://doi.org/10.12989/sem.2019.71.5.485.

Attia, A., Tounsi, A., AddaBedia, E.A., Mahmoud, S.R. (2015), "Free vibration analysis of functionally graded plates with temperature-dependent properties using various four variable refined plate theories", *Steel Compos. Struct*., **18**(1), 187-212. https://doi.org/10.12989/scs.2015.18.1.187.

Attia, A., Bousahla, A.A., Tounsi, A., Mahmoud, S.R., Alwabli, A.S. (2018), "A refined four variable plate theory for thermoelastic analysis of FGM plates resting on variable elastic foundations", *Struct. Eng. Mech*., **65**(4), 453-464. https://doi.org/10.12989/sem.2018.65.4.453.

Bakhadda, B., BachirBouiadjra, M., Bourada, F., Bousahla, A.A., Tounsi, A., Mahmoud, S.R. (2018), "Dynamic and bending analysis of carbon nanotube-reinforced composite plates with elastic foundation", *Wind Struct.*, **27**(5), 311-324. https://doi.org/10.12989/was.2018.27.5.31.

Barati, M. R., &Shahverdi, H. (2016), "A four-variable plate theory for thermal vibration of embedded FG nanoplates under non-uniform temperature distributions with different boundary conditions", *Struct. Eng. Mech.*, **60**(4), 707-727. https://doi.org/10.12989/sem.2016.60.4.707.

Belabed, Z., Bousahla, A.A., Houari, M.S.A., Tounsi, A., Mahmoud, S.R. (2018), "A new 3-unknown hyperbolic shear deformation theory for vibration of functionally graded sandwich plate", *Earthq. Struct.*, **14**(2), 103-115. https://doi.org/10.12989/eas.2018.14.2.103.

Beldjelili, Y., Tounsi, A., & Mahmoud, S.R. (2016), "Hygro-thermo-mechanical bending of S-FGM plates resting on variable elastic foundations using a four-variable trigonometric plate theory", *Smart Struct. Syst.*, **18**(4), 755-786. https://doi.org/10.12989/sss.2016.18.4.755.

Bellifa, H., Benrahou, K.H., Bousahla, A.A., Tounsi, A. and Mahmoud, S.R. (2017a), "A nonlocal zeroth-order shear deformation theory for nonlinear postbuckling of nanobeams", *Struct. Eng. Mech*., **62**(6), 695-702. https://doi.org/10.12989/sem.2017.62.6.695.

Bellifa, H., Bakora, A., Tounsi, A., Bousahla, A.A. and Mahmoud, S.R. (2017b), "An efficient and simple four variable refined plate theory for buckling analysis of functionally graded plates", *Steel Compos. Struct*., **25**(3), 257-270. https://doi.org/10.12989/scs.2017.25.3.257.

Benchohra, M., Driz, H., Bakora, A., Tounsi, A., AddaBedia, E.A. and Mahmoud, S.R. (2018), "A new quasi-3D sinusoidal shear deformation theory for functionally graded plates", *Struct. Eng. Mech*., **65**(1), 19-31. https://doi.org/10.12989/sem.2018.65.1.019.

Berghouti, H., AddaBedia, E.A. Benkhedda, A., Tounsi, A. (2019), "Vibration analysis of nonlocal porous nanobeams made of functionally graded material", *Adv. Nano Res.*, **7**(5), 351-364. https://doi.org/10.12989/anr.2019.7.5.351.

Bouadi, A., Bousahla, A.A., Houari, M.S.A., Heireche, H., Tounsi, A. (2018), "A new nonlocal HSDT for analysis of stability of single layer graphene sheet", *Adv. Nano Res.*, **6**(2), 147-162. https://doi.org/10.12989/anr.2018.6.2.147.

Bouiadjra, R. B., Bedia, E. A. and Tounsi, A. (2013), "Nonlinear thermal buckling behavior of functionally graded plates using an efficient sinusoidal shear deformation theory", *Struct. Eng. Mech.*, **48**(4), 547-567. https://doi.org/10.12989/sem.2013.48.4.547.

Bouhadra, A., Tounsi, A., Bousahla, A.A., Benyoucef, S., Mahmoud, S.R. (2018), "Improved HSDT accounting for effect of thickness stretching in advanced composite plates", *Struct. Eng. Mech*., **66**(1), 61-73. https://doi.org/10.12989/sem.2018.66.1.061.

Boukhlif, Z., Bouremana, M., Bourada, F., Bousahla, A.A., Bourada, M., Tounsi, A., Al-Osta, M.A. (2019), "A simple quasi-3D HSDT for the dynamics analysis of FG thick plate on elastic foundation", *Steel Compos. Struct.*, **31**(5), 503-516. https://doi.org/10.12989/scs.2019.31.5.503.

Boulefrakh, L., Hebali, H., Chikh, A., Bousahla, A.A., Tounsi, A., Mahmoud, S.R. (2019), "The effect of parameters of visco-Pasternak foundation on the bending and vibration properties of a thick FG plate", *Geomech. Eng.*, **18**(2), 161-178. https://doi.org/10.12989/gae.2019.18.2.161.

Bounouara, F., Benrahou, K.H., Belkorissat, I. and Tounsi, A. (2016), "A nonlocal zeroth-order shear deformation theory for free vibration of functionally graded nanoscale plates resting on elastic foundation", *Steel Compos. Struct.,***20**(2), 227-249. https://doi.org/10.12989/scs.2016.20.2.227.

Bourada, F., Bousahla, A.A., Bourada, M., Azzaz, A., Zinata, A., Tounsi, A. (2019), "Dynamic investigation of porous functionally graded beam using a sinusoidal shear deformation theory", *Wind Struct.*, **28**(1), 19-30. https://doi.org/10.12989/was.2019.28.1.019.

Bourada, F., Amara, K., Bousahla, A.A., Tounsi, A., Mahmoud, S.R. (2018), "A novel refined plate theory for stability analysis of hybrid and symmetric S-FGM plates", *Struct. Eng. Mech.*, **68**(6), 661-675. https://doi.org/10.12989/sem.2018.68.6.661.

Bousahla, A.A., Benyoucef, S., Tounsi, A. and Mahmoud, S.R. (2016), "On thermal stability of plates with functionally graded coefficient of thermal expansion," *Struct. Eng. Mech*., **60**(2), 313-335. https://doi.org/10.12989/sem.2016.60.2.313.

Boussoula, A.,Boucham, B., Bourada, M.,Bourada, F.,Tounsi, A.,Bousahla, A.A., Tounsi, A. (2019), "A simple nth-order shear deformation theory for thermomechanical bending analysis of different configurations of FG sandwich plates", *Smart Struct.*

Syst.., (In press).

Boutaleb, S., Benrahou, K.H., Bakora, A., Algarni, A., Bousahla, A.A., Tounsi, A., Mahmoud, S.R., Tounsi, A. (2019), "Dynamic Analysis of nanosize FG rectangular plates based on simple nonlocal quasi 3D HSDT", *Adv. Nano Res.*, **7**(3), 189-206. https://doi.org/10.12989/anr.2019.7.3.191.

Chaabane, L.A., Bourada, F., Sekkal, M., Zerouati, S., Zaoui, F.Z., Tounsi, A., Derras, A., Bousahla, A.A. and Tounsi, A. (2019), "Analytical study of bending and free vibration responses of functionally graded beams resting on elastic foundation", *Struct. Eng. Mech.*, **71**(2), 185-196. https://doi.org/10.12989/sem.2019.71.2.185.

Chemi, A., Zidour, M., Heireche, H., Rakrak, K., & Bousahla, A. A. (2018). "Critical buckling load of chiral double-walled carbon nanotubes embedded in an elastic medium", *Mech. Compos. Mater.*, **53**(6), 827-836. https://doi.org/10.1007/s11029-018-9708-x.

Cherif, R.H., Meradjah, M., Zidour, M., Tounsi, A., Belmahi, H. and Bensattalah, T. (2018), "Vibration analysis of nano beam using differential transform method including thermal effect", *J. Nano Res.*, **54**, 1-14. https://doi.org/10.4028/www.scientific.net/JNanoR.54.1.

Chikh, A., Tounsi, A., Hebali, H. and Mahmoud, S.R. (2017), "Thermal buckling analysis of cross-ply laminated plates using a simplified HSDT", *Smart Struct. Syst*., **19**(3), 289-297. https://doi.org/10.12989/sss.2017.19.3.289.

Coleman, J. N., Khan, U., Blau, W. J., and Gunko, Y. K., (2006), "Small but Strong: A Review of the Mechanical Properties of Carbon Nanotube-polymer Composites", *Carbon*, **44**, 1624–1652. https://doi.org/10.1016/j.carbon.2006.02.038.

Dehghan, M., &Abbaszadeh, M. (2016), "Proper orthogonal decomposition variationalmultiscale element free Galerkin (POD-VMEFG) meshless method for solving incompressible Navier–Stokes equation", *Comput. Method. Appl. Mech. Eng.*, **311**, 856-888. https://doi.org/10.1016/j.cma.2016.09.008.

Dehghan, M. and Abbaszadeh, M. (2019), "The solution of nonlinear Green–Naghdi equation arising in water sciences via a meshless method which combines moving kriging interpolation shape functions with the weighted essentially non–oscillatory method", *Communications in Nonlinear Sci. Numerical Simulation*, **68**, 220-239. https://doi.org/10.1016/j.cnsns.2018.07.029.

Dehghan, M., Abbaszadeh, M. and Mohebbi, A. (2016), "Legendre spectral element method for solving time fractional modified anomalous sub-diffusion equation", *Appl. Math. Modelling*, **40**(5-6), 3635-3654. https://doi.org/10.1016/j.apm.2015.10.036.

Dehghan, M. and Baradaran, G.H. (2011), "Buckling and free vibration analysis of thick rectangular plates resting on elastic foundation using mixed finite element and differential quadrature method", *Appl. Math. Comput.*, **218**, 2772–2784. https://doi.org/10.1016/j.amc.2011.08.020.

Dehghan, M. and Mohammadi, V. (2015a), "The method of variably scaled radial kernels for solving two-dimensional magnetohydrodynamic (MHD) equations using two discretizations: The Crank–Nicolson scheme and the method of lines (MOL)", *Comput. Math. Appl.*, **70**(10), 2292-2315. https://doi.org/10.1016/j.camwa.2015.08.032.

Dehghan, M. and Mohammadi, V. (2015b), "The method of variably scaled radial kernels for solving two-dimensional magnetohydrodynamic (MHD) equations using two discretizations: the Crank–Nicolson scheme and the method of lines (MOL)", *Comput. Math. Appl.*, **70**(10), 2292-2315. https://doi.org/10.1016/j.camwa.2015.08.032.

Dehghan, M. and Shokri, A. (2008), "A numerical method for solution of the two-dimensional sine-Gordon equation using the radial basis functions", *Math. Comput. Simulation*, **79**(3), 700-715. https://doi.org/10.1016/j.matcom.2008.04.018.

Dihaj, A., Zidour, M., Meradjah, M., Rakrak, K., Heireche, H., and Chemi, A. (2018), "Free vibration analysis of chiral double-walled carbon nanotube embedded in an elastic medium using non-local elasticity theory and Euler Bernoulli beam model", *Struct. Eng. Mech.*, **65(**3), 335-342. https://doi.org/10.12989/sem.2018.65.3.335.

Draiche, K., Tounsi, A. and Mahmoud, S.R. (2016), "A refined theory with stretching effect for the flexure analysis of laminated composite plates", *Geomech. Eng*., **11**(5), 671-690. https://doi.org/10.12989/gae.2016.11.5.671.

Draiche, K., Bousahla, A.A., Tounsi, A., Alwabli, A.S., Tounsi, A. and Mahmoud, S.R. (2019), "Static analysis of laminated reinforced composite plates using a simple first-order shear deformation theory", *Comput. Concrete*, **24**(4), 369-378. https://doi.org/10.12989/cac.2019.24.4.369.

Draoui, A., Zidour, M., Tounsi, A. and Adim, B. (2019), "Static and dynamic behavior of nanotubes-reinforced sandwich plates using (FSDT)", *J. Nano Res.*, **57**, 117-135. https://doi.org/10.4028/www.scientific.net/JNanoR.57.117.

El-Haina, F., Bakora, A., Bousahla, A.A., Tounsi, A. and Mahmoud, S.R. (2017), "A simple analytical approach for thermal buckling of thick functionally graded sandwich plates", *Struct. Eng. Mech*., **63**(5), 585-595. https://doi.org/10.12989/sem.2017.63.5.585.

Fadelus, J.D., Wiesel, E., Gojny, F.H., Schulte, K., Wagner, H.D. (2005), "Thermo-mechanical properties of randomly oriented carbon/epoxy nanocomposites", *Compos. Part A*, **36**, 1555-1561. https://doi.org/10.1016/j.compositesa.2005.02.006.

Fourn, H., AitAtmane, H., Bourada, M., Bousahla, A.A., Tounsi, A. and Mahmoud, S.R. (2018), "A novel four variable refined plate theory for wave propagation in functionally graded material plates", *Steel Compos. Struct.*, **27**(1), 109-122. https://doi.org/10.12989/scs.2018.27.1.109.

Guessas, H., Zidour, M., Meradjah, M. and Tounsi, A. (2018), "The critical buckling load of reinforced nanocomposite porous plates", *Struct. Eng. Mech.*, **67**(2), 115-123. https://doi.org/10.12989/sem.2018.67.2.115.

Hamidi, A., Zidour, M., Bouakkaz, K. and Bensattalah, T. (2018), "Thermal and Small-Scale Effects on Vibration of Embedded Armchair Single-Walled Carbon Nanotubes", *J. Nano Res.,* **51**, 24-38. https://doi.org/10.4028/www.scientific.net/JNanoR.51.24.

Han, Y., Elliott, J., (2007), "Molecular dynamics simulations of the elastic properties of polymer/carbon nanotube composites", *Comput. Mater. Sci*., **39**, 315-323. https://doi.org/10.1016/j.commatsci.2006.06.011.

Hellal, H., Bourada, M., Hebali, H., Bourada, F., Tounsi, A., Bousahla, A.A. and Mahmoud, S.R. (2019), "Dynamic and stability analysis of functionally graded material sandwich plates in hygro-thermal environment using a simple higher shear deformation theory", *J. Sandwich Struct. Mater.*, https://doi.org/10.1177/1099636219845841.

Hoang V. T., (2016), "Thermal buckling and postbuckling behavior of functionally graded carbon-nanotube-reinforced composite plates resting on elastic foundations with tangential-edge restraints", *J. Thermal Stress.*, https://doi.org/10.1080/01495739.2016.1254577.

Hu, N., Fukunaga, H., Lu, C., Kameyama, M. and Yan. B. (2005), "Prediction of elastic properties of carbon nanotube reinforced composites", *Proc. Royal Soc. A*, **461**, 1685-1710. https://doi.org/10.1098/rspa.2004.1422.

Hussain, M., Naeem, M.N., Tounsi, A. and Taj, M. (2019), "Nonlocal effect on the vibration of armchair and zigzag SWCNTs with bending rigidity", *Adv. Nano Res.*, **7**(6), 431-432. https://doi.org/10.12989/anr.2019.7.6.431.

Ilati, M. and Dehghan, M. (2015), "The use of radial basis functions (RBFs) collocation and RBF-QR methods for solving the coupled nonlinear sine-Gordon equations", *Eng. Analysis*

Boundary Elements, **52**, 99-109. https://doi.org/10.1016/j.enganabound.2014.11.023.

Kaci, A., Houari, M.S.A., Bousahla, A.A., Tounsi, A. and Mahmoud, S.R. (2018), "Post-buckling analysis of shear-deformable composite beams using a novel simple two-unknown beam theory", *Struct. Eng. Mech.*, **65**(5), 621-631. https://doi.org/10.12989/sem.2018.65.5.621.

Karami, B., Janghorban, M. and Tounsi, A. (2019a), "On exact wave propagation analysis of triclinic material using three dimensional bi-Helmholtz gradient plate model", *Struct. Eng. Mech.*, **69**(5), 487-497. https://doi.org/10.12989/sem.2019.69.5.487.

Karami, B., Janghorban, M., Tounsi, A. (2019b), "Wave propagation of functionally graded anisotropic nanoplates resting on Winkler-Pasternak foundation", *Struct. Eng. Mech.*, **7**(1), 55-66. https://doi.org/10.12989/sem.2019.70.1.055.

Karami, B., Shahsavari, D., Janghorban, M., Tounsi, A. (2019c), "Resonance behavior of functionally graded polymer composite nanoplates reinforced with grapheme nanoplatelets", *J. Mech. Sci.*, **156**, 94-105. https://doi.org/10.1016/j.ijmecsci.2019.03.036.

Karami, B., Janghorban, M. and Tounsi, A. (2019d), "Galerkin's approach for buckling analysis of functionally graded anisotropic nanoplates/different boundary conditions", *Eng. Comput.*, **35**, 1297-1316. https://doi.org/10.1007/s00366-018-0664-9.

Karami, B., Janghorban, M. and Tounsi, A. (2018a), "Variational approach for wave dispersion in anisotropic doubly-curved nanoshells based on a new nonlocal strain gradient higher order shell theory", *Thin Wall. Struct.*, **129**, 251–264. https://doi.org/10.1016/j.tws.2018.02.025.

Karami, B., Janghorban, M., Shahsavari, D. and Tounsi, A. (2018b), "A size-dependent quasi-3D model for wave dispersion analysis of FG nanoplates", *Steel Compos. Struct.*, **28**(1), 99-110. https://doi.org/10.12989/scs.2018.28.1.099.

Karami, B., Janghorban, M. and Tounsi, A. (2018c), "Nonlocal strain gradient 3D elasticity theory for anisotropic spherical nanoparticles", *Steel Compos. Struct.*, **27**(2), 201-216. https://doi.org/10.12989/scs.2018.27.2.201.

Karami, B., Janghorban, M. and Tounsi, A. (2017), "Effects of triaxial magnetic field on the anisotropic nanoplates", *Steel Compos. Struct.*, **25**(3), 361-374. https://doi.org/10.12989/scs.2017.25.3.361.

Ke, L.L., Yang, J. and Kitipornchai, S. (2010), "Nonlinear free vibration of functionally graded carbon nanotube-reinforced composite beams", *Compos. Struct.*, **92**, 676-683. https://doi.org/10.1016/j.compstruct.2009.09.024.

Kerr, A.D. (1964), "Elastic and viscoelastic foundation models", *J. Appl. Mech.*, **31**(3), 491-498. https://doi.org/10.1115/1.3629667.

Kerr, A.D. (1965), "A study of a new foundation model", *Acta Mechanica*, **1**(2), 135-147. https://doi.org/10.1007/BF01174308.

Khayat, M., Dehghan, S. M., Najafgholipour, M. A. and Baghlani, A. (2018), "Free vibration analysis of functionally graded cylindrical shells with different shell theories using semi-analytical method", *Steel Compos. Struct.*, **28**(6), 735-748. https://doi.org/10.12989/scs.2018.28.6.735.

Khiloun, M., Bousahla, A.A., Kaci, A., Bessaim, A., Tounsi, A., Mahmoud, S.R. (2019), "Analytical modeling of bending and vibration of thick advanced composite plates using a four-variable quasi 3D HSDT", *Eng. Comput.*, https://doi.org/10.1007/s00366-019-00732-1.

Kolahchi, R., Bidgoli, M.R., Beygipoor, G. and Fakhar, M.H. (2015), "A nonlocal nonlinear analysis for buckling in embedded FG-SWCNT-reinforced microplates subjected to magnetic field", *J. Mech. Sci. Technol.*, **29**(9), 3669-3677. https://doi.org/10.1007/s12206-015-0811-9.

Kolahchi, R., Zarei, M.S., Hajmohammad, M.H. and Nouri, A. (2017), "Wave propagation of embedded viscoelastic FG-CNT-reinforced sandwich plates integrated with sensor and actuator based on refined zigzag theory", *J. Mech. Sci.*, **130**, 534–545. https://doi.org/10.1016/j.ijmecsci.2017.06.039.

Lei, Z.X., Liew, K.M. and Yu, J.L. (2013), "Buckling analysis of functionally graded carbon nanotube reinforced composite plates using the element-free kp-Ritz method", *Compos. Struct.*, **98**, 160-168. https://doi.org/10.1016/j.compstruct.2012.11.006.

Mahi, A., AddaBedia, E.A. and Tounsi, A. (2015), "A new hyperbolic shear deformation theory for bending and free vibration analysis of isotropic, functionally graded, sandwich and laminated composite plates", *Appl. Math. Modelling.*, **39**(9), 2489-2508. https://doi.org/10.1016/j.apm.2014.10.045.

Mahmoudi *et al*. (2019), "A refined quasi-3D shear deformation theory for thermo-mechanical behavior of functionally graded sandwich plates on elastic foundations", *J. Sandwich Struct. Mater.*, **21**(6), 1906-1929. https://doi.org/10.1177/1099636217727577.

Medani, M., Benahmed, A., Zidour, M., Heireche, H., Tounsi, A., Bousahla, A.A., Tounsi, A. and Mahmoud, S.R. (2019), "Static and dynamic behavior of (FG-CNT) reinforced porous sandwich plate", *Steel Compos. Struct.*, **32**(5), 595-610. https://doi.org/10.12989/scs.2019.32.5.595.

Mehar, K, Panda, S.K. and Mahapatra, T.R. (2017), "Thermoelastic nonlinear frequency analysis of CNT reinforced functionally graded sandwich structure", *European J. Mech. A Solids*, **65**, 384-396. https://doi.org/10.1016/j.euromechsol.2017.05.005.

Mehar, K. and Panda, S.K. (2017), "Thermoelastic analysis of FG-CNT reinforced shear deformable composite plate under various loading", *J. Comput. Methods*, **14**(2), 1750019. https://doi.org/10.1142/S0219876217500190.

Meksi, R, Benyoucef, S., Mahmoudi, A., Tounsi, A., Adda Bedia, E.A. and Mahmoud, S.R. (2019), "An analytical solution for bending, buckling and vibration responses of FGM sandwich plates", *J. Sandw. Struct. Mater.*, **21**(2), 727-757. https://doi.org/10.1177%2F1099636217698443.

Menasria, A., Bouhadra, A., Tounsi, A., Bousahla, A.A. and Mahmoud, S.R. (2017), "A new and simple HSDT for thermal stability analysis of FG sandwich plates", *Steel Compos. Struct.*, **25**(2), 157-175. https://doi.org/10.12989/scs.2017.25.2.157.

Meziane, M.A.A., Abdelaziz, H.H. and Tounsi, A. (2014), "An efficient and simple refined theory for buckling and free vibration of exponentially graded sandwich plates under various boundary conditions", *J. Sandwich Struct. Mater.*, **16**(3), 293–318. https://doi.org/10.1177/1099636214526852.

Mokashi, V.V., Qian, D. and Liu, Y.J. (2007), "A study on the tensile response and fracture in carbon nanotube-based composites using molecular mechanics", *Compos. Sci. Technol*. **67**, 530-540. https://doi.org/10.1016/j.compscitech.2006.08.014.

Mokhtar, Y., Heireche, H., Bousahla, A.A., Houari, M.S.A., Tounsi, A. and Mahmoud, S.R. (2018), "A novel shear deformation theory for buckling analysis of single layer graphene sheet based on nonlocal elasticity theory", *Smart Struct. Syst.*, **21**(4), 397-405. https://doi.org/10.12989/sss.2018.21.4.397.

Moradi-Dastjerdi, R. (2016), "Wave propagation in functionally graded composite cylinders reinforced by aggregated carbon nanotube", *Struct. Eng. Mech.*, **57**(3), 441-456. https://doi.org/10.12989/sem.2016.57.3.441.

Nguyen DinhDuc, Jaehong Lee, T. Nguyen-Thoi, Pham ToanThang (2017), "Static response and free vibration of functionally graded carbon nanotube-reinforced composite rectangular plates resting on Winkler–Pasternak elastic foundations", *Aerosp. Sci. Technol.*, **68**, 391-402. https://doi.org/10.1016/j.ast.2017.05.032.

Odegard, G.M., Gates, T.S., Wise, K.E., Park, C. and Siochi, E.J. (2003), "Constitutive modelling of nanotube-reinforced polymer composites", *Compos. Sci. Technol*., **63**, 1671-1687.

Pradhan, S.C. and Phadikar, J.K. (2009), "Bending, buckling and vibration analyses of nonhomogeneous nanotubes using GDQ and nonlocal elasticity theory", *Struct. Eng. Mech.*, **33**(2), 193-213. https://doi.org/10.12989/sem.2009.33.2.193.

Rakrak, K., Zidour, M., Heireche, H., Bousahla, A. A. and Chemi, A. (2016), "Free vibration analysis of chiral double-walled carbon nanotube using non-local elasticity theory", *Adv. Nano Res.*, **4**(1), 31-44. https://doi.org/10.12989/anr.2016.4.1.031.

Shafiei, H. and Setoodeh, A.R. (2017), "Nonlinear free vibration and post-buckling of FG-CNTRC beams on nonlinear foundation", *Steel Compos. Struct.*, **24**(1), 65-77.

Shen, H.S. and Zhang, C.L. (2010), "Thermal buckling and postbuckling behavior of functionally graded carbon nanotube-reinforced composite plates", *Mater. Des.*, **31**, 3403-3411. https://doi.org/10.1016/j.matdes.2010.01.048.

Shen, H.S. (2009), "Nonlinear bending of functionally graded carbon nanotube reinforced composite plates in thermal environments", *Compos Struc*t., **91**, 9-19. https://doi.org/10.1016/j.compstruct.2009.04.026.

Shen H-S, Zhu, Z.H. (2012), "Postbuckling of sandwich plates with nanotube-reinforced composite face sheets resting on elastic foundations", *European J. Mech. A/Solids,* **35**, 10-21. https://doi.org/10.1016/j.euromechsol.2012.01.005.

Shokravi, M. (2017), "Buckling of sandwich plates with FG-CNT-reinforced layers resting on orthotropic elastic medium using Reddy plate theory", *Steel Compos. Struct.*, **23**, 623-631. https://doi.org/10.12989/scs.2017.23.6.623.

Spitalsky, Z., Tasis, D., Papagelis, K., and Galiotis, C. (2010), "Carbon Nanotube-polymer Composites: Chemistry, Processing, Mechanical and Electrical Properties", *Prog. Polym. Sci.*, **35**, 357–401. https://doi.org/10.1016/j.progpolymsci.2009.09.003.

Thai, H.T., Choi, D.H., (2011), "A refined plate theory for functionally graded plates resting on elastic foundation", *Compo. Sci. Tech.* **71**, 1850-1858. https://doi.org/10.1016/j.compscitech.2011.08.016.

Tlidji, Y., Zidour, M., Draiche, K., Safa, A., Bourada, M., Tounsi, A., Bousahla, A. A., and Mahmoud, S.R., (2019) "Vibration analysis of different material distributions of functionally graded microbeam", *Struct. Eng. Mech.*, **69**(6), 637-649. https://doi.org/10.12989/sem.2019.69.6.637.

Vancauwelaert, F., Stet, M. and Jasieskia, A. (2002), "The general solution for a slab subjected to center and edge loads and resting on a Kerr foundation", *J. Pavement Eng.*, **3**(1), 1-18. https://doi.org/10.1080/10298430290029894.

Wattanasakulpong, N. and Ungbhakorn, V. (2013), "Analytical solutions for bending, buckling and vibration responses of carbon nanotube-reinforced composite beams with elastic foundation", *Comput. Mater. Sci.*, **71**, 201-208. https://doi.org/10.1016/j.commatsci.2013.01.028.

Wattanasakulpong, N. and Chaikittiratana, A. (2015), "Exact solutions for static and dynamic analyses of carbon nanotube-reinforced composite plates with Pasternak elastic foundation", *Appl. Math. Modelling*, **39**(18), 5459-5472. https://doi.org/10.1016/j.apm.2014.12.058.

Winkler, E. (1867), *Die Lehre von der Elasticitaet und Festigkeit: mitbesondererRücksicht auf ihreAnwendung in der TechnikfürpolytechnischeSchulen, Bauakademien, Ingenieue, Maschinenbauer, Architecten, etc.,* Volume 1, Dominicus, Germany.

Xie, X.L., Mai, Y.W. and Zhou, X.P. (2005), "Dispersion and alignment of carbon nanotubes in polymer matrix: A review", *Mater. Sci. Eng.*, **49**, 89-112. https://doi.org/10.1016/j.mser.2005.04.002.

Yas, M.H. and Samadi N. (2012), "Free vibration and buckling analysis of carbon nanotube-reinforced composite Timoshenko beams on elastic foundation", *Int. J. Press.Ves.Pip.*, **98**, 119-128. https://doi.org/10.1016/j.ijpvp.2012.07.012.

Yazid, M., Heireche, H., Tounsi, A., Bousahla, A.A. and Houari, M.S.A. (2018), "A novel nonlocal refined plate theory for stability response of orthotropic single-layer graphene sheet resting on elastic medium", *Smart Struct. Syst..*, **21**(1), 15-25. https://doi.org/10.12989/sss.2018.21.1.015.

Youcef, D.O., Kaci, A., Benzair, A., Bousahla, A.A. and Tounsi, A. (2018), "Dynamic analysis of nanoscale beams including surface stress effects", *Smart Struct. Syst..*, **21**(1), 65-74. https://doi.org/10.12989/sss.2018.21.1.065.

Younsi, A., Tounsi, A, Zaoui, F.Z., Bousahla, A.A. and Mahmoud, S.R. (2018), "Novel quasi-3D and 2D shear deformation theories for bending and free vibration analysis of FGM plates", *Geomech. Eng.*, **14**(6), 519-532. https://doi.org/10.12989/gae.2018.14.6.519.

Zaoui, F.Z., Ouinas, D. and Tounsi, A. (2019), "New 2D and quasi-3D shear deformation theories for free vibration of functionally graded plates on elastic foundations", *Compos. Part B*, **159**, 231-247. https://doi.org/10.1016/j.compositesb.2018.09.051.

Zarga, D., Tounsi, A., Bousahla, A.A., Bourada, F. and Mahmoud, S.R. (2019), "Thermomechanical bending study for functionally graded sandwich plates using a simple quasi-3D shear deformation theory", *Steel Compos. Struct.*, **32**(3), 389-410. https://doi.org/10.12989/scs.2019.32.3.389.

Zenkour, A.M., (2006), "Generalized shear deformation theory for bending analysis of functionally graded plates", *Appl. Math. Model.*, **30**, 67-84. https://doi.org/10.1016/j.apm.2005.03.009.

Zenkour, A.M., (2009), "The refined sinusoidal theory for FGM plates on elastic foundations", *Int. J. Mech. Sci.,* **51**, 869-880. https://doi.org/10.1016/j.ijmecsci.2009.09.026.

Zhang, L.W., Lei, Z.X. and Liew, K.M. (2015), "Computation of vibration solution for functionally graded carbon nanotube-reinforced composite thick plates resting on elastic foundations using the element-free IMLS-Ritz method", *Appl. Math. Comput.*, **256**, 488–504. https://doi.org/10.1016/j.amc.2015.01.066.

Zhou, D., Cheung, Y.K., Lo, S.H. and Au, F.T.K. (2004), "Three-dimensional vibration analysis of rectangular thick plates on Pasternak foundation", *Int. J. Numer. Methods Eng.*, **59**, 1313–1334. https://doi.org/10.1002/nme.915.

Zhu, R., Pan, E. and Roy, A.K. (2007), "Molecular dynamics study of the stress-strain behavior of carbon- nanotube reinforced Epon 862 composites", *Mater. Sci. Eng. A*, **447**, 51-57. https://doi.org/10.1016/j.msea.2006.10.054.

Zhu, P., Lei, Z.X. and Liew, K.M. (2012), "Static and free vibration analyses of carbon nanotube reinforced composite plates using finite element method with first order shear deformation plate theory", *Compos. Struct*. **94**, 1450-1460. https://doi.org/10.1016/j.compstruct.2011.11.010.

Zine, A., Tounsi, A., Draiche, K., Sekkal, M. and Mahmoud, S.R. (2018), "A novel higher-order shear deformation theory for bending and free vibration analysis of isotropic and multilayered plates and shells", *Steel Compos. Struct.*, **26**(2), 125-137. https://doi.org/10.12989/scs.2018.26.2.125.

CC